Fuel 143 (2015) 318–326

Contents lists available at ScienceDirect

Fuel

journal homepage: www.elsevier.com/locate/fuel

Ru/TiO_2 for the preferential oxidation of CO in H_2-rich stream: Effects of catalyst pre-treatments and reconstruction of Ru sites

Lu Di, Guangjun Wu, Weili Dai, Naijia Guan, Landong Li *

Collaborative Innovation Center of Chemical Science and Engineering (Tianjin) & Key Laboratory of Advanced Energy Materials Chemistry of Ministry of Education, College of Chemistry, Nankai University, Tianjin 300071, China

HIGHLIGHTS

- Ru/TiO_2 exhibits remarkable catalytic performance in the reaction of CO PROX for fuel cell application.
- The catalyst preparation and pre-treatment show great impacts on the catalytic performance.
- Isolated metallic Ru species are identified as preferred active sites in CO PROX.
- Linear monocarbonyls are determined to be key reaction intermediates in CO PROX.

ARTICLE INFO

Article history:
Received 14 October 2014
Received in revised form 9 November 2014
Accepted 16 November 2014
Available online 3 December 2014

Keywords:
Preferential oxidation
Ru/TiO_2
Pre-treatment
Reconstruction

ABSTRACT

The preferential oxidation (PROX) of CO is a promising strategy for trace CO clean up in H_2-rich stream to fuel cells. In the present study, a series of TiO_2 supported clusters were prepared and studied for the PROX of CO. Amongst, Ru/TiO_2 catalyst exhibited remarkably high PROX activity in the operation temperature range of fuel cells. The effects of catalyst preparation and pre-treatment on the catalytic performance of Ru/TiO_2 were investigated in detail. Ru/TiO_2 catalyst prepared by photo-deposition and pre-treated under H_2–CO atmosphere was found to be the most promising one and complete CO oxidation could be achieved at >373 K. Ru/TiO_2 pre-treated under different reducing atmospheres were characterized by high-resolution transmission electron microscopy (HRTEM), X-ray photoelectron spectroscopy (XPS) and Fourier transform infrared spectroscopy (FTIR) of CO adsorption. The surface reconstruction of Ru sites during catalyst pre-treatment was observed and isolated metallic Ru species was identified as preferred active sites for PROX reaction. Based on the catalytic and characterization results, the possible mechanism for PROX of CO over Ru/TiO_2 was proposed.

1. Introduction

In the past decades, extensive attention has been focused on hydrogen as a clean energy resource and ideal energy carrier, which can be applied in fuel cells, e.g. polymer electrolyte membrane fuel cell (PEMFC), to produce electricity efficiently and free of associative pollutants [1–3]. The current large-scale hydrogen source is co-produced with significant amounts of carbon monoxide via the steam reforming and partial oxidation of methane, and carbon monoxide is known as a conventional contaminant to be removed. Although a subsequent water–gas-shift (WGS) reaction can reduce the amount of carbon monoxide to 1%, even low levels of carbon monoxide contained in fuel hydrogen will do great harm to the anodes of fuel cell, e.g. Pt and Pt-based alloys in PEMFC, at low temperatures, i.e. 353–393 K [4–7]. Thus, it is essential to eliminate trace amounts of carbon monoxide from the reformate stream prior to its introduction into the fuel cell. Several different approaches, such as the selective diffusion, the selective carbon monoxide methanation and preferential oxidation (PROX) of carbon monoxide, have been proposed for the elimination of trace carbon monoxide in hydrogen stream. Among the above-mentioned approaches, PROX appears to be feasible for trace carbon monoxide clean up or bringing down the carbon monoxide concentration from 1% to acceptable level, i.e. below 20 ppm [8,9]. To date, various catalysts, e.g. platinum group metal catalysts [10–14], supported Au catalysts [15,16] and transition metal oxides-based catalysts [17–19], have been explored aiming to improve the carbon monoxide elimination with simultaneous minimizing the loss of hydrogen.

Supported Ru catalysts have been acknowledged as promising candidates for application in PROX due to their outstanding

* Corresponding author. Tel./fax: +86 22 2350 0341.
E-mail address: lild@nankai.edu (L. Li).

http://dx.doi.org/10.1016/j.fuel.2014.11.045
0016-2361/

activity and selectivity [20–22], however, superior Ru catalysts with enhanced PROX performance are still being explored. Moreover, the PROX performance of Ru catalysts is well debated probably due to the impacts from catalyst constitutions, preparation procedures and catalyst pre-treatment conditions, which consequently leads to an unsatisfying reproducibility for commercial application.

In the present study, a highly-active Ru/TiO_2 catalyst will be optimized for the PROX of carbon monoxide and researches will be focus on the unexpected effects of catalyst pretreatment conditions on their catalytic performance. The structure and electronic state of Ru/TiO_2 catalysts are well characterized by means of high-resolution transmission electron microscopy (HRTEM), X-ray photoelectron spectroscopy (XPS) and Fourier transform Infrared spectroscopy (FTIR) with carbon monoxide adsorption. Based on the results, the surface reconstruction of Ru sites during catalyst pre-treatment can be concluded and the structure–activity relationship of Ru/TiO_2 in PROX will be proposed, which is of great significance for future catalyst design.

2. Experimental

2.1. Preparation of Me/TiO_2 catalysts

Commercial TiO_2 (Degussa P25, 70% anatase, 30% rutile) was used as support and Me/TiO_2 (Me = Cu, Co, Mn, Ru, Au, Ir, Ag, Pt and Pd) catalysts with different metal loadings were prepared by so-called photo-deposition method [23]. The efficiency of photo-deposition is approaching 100% and the actual loadings of metals on TiO_2 are almost identical to the desired loadings, i.e. within measuring errors of ±2%. In a typical preparation of 1% Ru/TiO_2, 2 mM $RuCl_3$ solution containing 5 mg Ru, 500 mg TiO_2 and 8 mL of methanol were added into a round-bottom quartz flask under stirring to form slurry. The slurry was adjusted to pH 10 ± 0.5 using either 1 M HCl or 1 M NaOH aqueous solution and irradiated by a high-pressure mercury light with the main wavelength of 365 nm for 6 h under the protection of pure nitrogen. Finally, the particles were filtered, dried at ambient conditions and denoted as Ru/TiO_2-p.

For reference, 1% Ru/TiO_2 samples were also prepared by wet impregnation and chemical reduction methods. For wet impregnation, 2 mM $RuCl_3$ solution containing 5 mg Ru was added to 500 mg of TiO_2 and then the mixture was evaporated in a rotary evaporator at constant temperature of 353 K. The as-obtained particles were carefully washed with deionized water, dried at ambient conditions, and denoted as Ru/TiO_2-i. For chemical reduction, 500 mg of TiO_2 and 2 mM $RuCl_3$ solution containing 5 mg Ru were added into a round-bottom quartz flask under stirring to form slurry. Then 10 mL of 1 M KBH_4 solution was dropwise added to the slurry under the protection of nitrogen. The particles were filtered, washed with deionized water, dried at ambient conditions and denoted as Ru/TiO_2-c.

The as-prepared Ru/TiO_2 samples were calcined in flowing air at 523 K for 1 h and then subjected to different pre-treatments prior to being used as catalysts in PROX. The pre-treatments were performed at 523 K for 1 h under reducing atmospheres, i.e. 60% H_2 in He (H_2), 1% CO in He (CO) and 1% CO–60% H_2 in He (H_2–CO).

2.2. Catalyst characterization

HRTEM images of samples were acquired by a Philips Tecnai G20 S-TWIN electron microscope at an acceleration voltage of 200 kV. A few drops of alcohol suspension containing the samples were placed on a carbon-coated copper grid, followed by evaporation at ambient temperature.

XPS were recorded on a Kratos Axis Ultra DLD spectrometer with a monochromated Al Kα X-ray source ($h\nu$ = 1486.6 eV), hybrid (magnetic/electrostatic) optics and a multi-channel plate and delay line detector (DLD). All spectra were recorded by using an aperture slot of 300 × 700 microns. Survey spectra were recorded with a pass energy of 160 eV and high-resolution spectra with a pass energy of 40 eV. Accurate binding energies (±0.1 eV) were determined with respect to the position of the adventitious C 1s peak at 284.8 eV.

FTIR spectra of CO adsorption on Ru/TiO_2 samples were collected on the Bruker Tensor 27 spectrometer with 128 scans at a resolution of 4 cm^{-1}. A self-supporting pellet made of sample was placed in the IR flow cell and the reference spectrum, i.e. background spectrum, was taken at different temperatures. After the He stream was switched to a gas mixture containing 1% CO in He at a total flow rate of 30 mL min^{-1}, a series of time-dependent FTIR spectra of CO adsorption on the samples were sequentially recorded at designated temperatures.

The dispersion of ruthenium on TiO_2 support was determined by CO pulse adsorption on a chemisorption analyzer (Chemisorb 2720, Micromeritics). In a typical experiment, ca. 100 mg sample in the quartz reactor was first reduced in different atmospheres and purged in He at 523 K for 1 h to remove physisorbed molecules on the surface. After cooling down to room temperature in flowing He, pulses of 5%CO/He were injected to the reactor one pulse per minute until no further changes in signal intensity of outlet CO. The dispersion of ruthenium was calculated assuming the equimolar adsorption of CO on ruthenium metal [24].

In situ FTIR spectroscopy studies were performed on the Bruker Tensor 27 spectrometer by using a diffuse reflectance attachment equipped with a reaction chamber (Harrick, Praying Mantis CHC-CHA-3). 128 single beam spectra had been co-added at a resolution of 4 cm^{-1} and the spectra were presented as Kubelka–Munk function referred to adequate background spectra. The samples were used as self-supporting wafers (ca. 20 mg) and pretreated under different atmospheres at 523 K for 1 h prior to adsorption experiments. After cooling to desired temperature in flowing He, the stream was switched to reactant gas mixture and steady-state FTIR spectra were recorded after time-on-stream of 30 min.

2.3. Catalytic evaluation

The PROX reaction was performed in a fixed-bed flow microreactor at atmospheric pressure. Typically, 0.2 g catalyst (sieve fraction, 0.25–0.5 mm) was placed in a quartz reactor (4 mm i.d.) and pretreated under different conditions. After cooling down to 323 K in flowing He, the reactant gas mixture (1% CO, 1% O_2, 60% H_2 in He) was fed to the reactor. The total flow rate of the gas mixture was kept at 75 mL min^{-1}, corresponding to a GHSV of 22, 500 h^{-1}. The inlet and outlet gases were analyzed on-line by using a Varian CP 3800 gas chromatograph (TCD detector and with molecular sieve 5A and Porapak Q columns for H_2, O_2, CO and CO_2 analysis). Under our reaction conditions, i.e. at relatively low reaction temperatures and in the presence oxygen, the methanation of CO does not occur. Accordingly, the CO conversion and the CO_2 selectivity are calculated based on following equations.

$$\text{CO conversion}: X_{CO} = \frac{[CO]_{inlet} - [CO]_{outlet}}{[CO]_{inlet}} \times 100\%; \quad (1)$$

$$O_2 \text{ conversion}: X_{O_2} = \frac{[O_2]_{inlet} - [O_2]_{outlet}}{[O_2]_{inlet}} \times 100\%; \quad (2)$$

$$CO_2 \text{ selectivity}: S_{CO_2} = \frac{X_{CO}}{2 \times X_{O_2}} \times 100\%. \quad (3)$$

3. Results and discussion

3.1. PROX of carbon monoxide catalyzed by Me/TiO_2

Fig. 1 shows the PROX of carbon monoxide over a series of TiO_2 supported catalysts in the feed stream composition of 1% CO, 1% O_2 and 60% H_2 in He balance. Ru/TiO_2 exhibits the highest activity at low temperatures, i.e. below 393 K, while Cu/TiO_2 and Co/TiO_2 exhibit good activity at high temperatures, i.e. over 393 K (all catalysts pre-treated in 60%H_2/He at 523 K for 1 h, the catalytic activity obtained should be dependent on the catalyst preparation method, active metal loading and catalyst pre-treatment conditions). Considering the target application in CO elimination for fuel cells, i.e. reducing CO from 1% to below 100 ppm, Ru/TiO_2 is undoubtedly the most promising candidate with TiO_2 as support material. Typically, CO conversion of *ca.* 80% could be obtained at 393 K with CO_2 selectivity of *ca.* 40% (under our reaction conditions, the reverse water gas shift reaction did not occur), consistent with literature reports on other Ru catalysts under similar reaction conditions. Consequently, a detailed study will focus on Ru/TiO_2 as a model catalyst in the following section.

3.2. PROX of carbon monoxide catalyzed by Ru/TiO_2

Fig. 2 shows the PROX behaviors of Ru/TiO_2 catalysts prepared by different methods and pre-treated under different reducing atmospheres, respectively. It is obvious that both preparation methods and pre-treatment conditions show great impacts on the PROX performance of Ru/TiO_2, which should be explained from the different Ru–TiO_2 interaction obtained. Generally, Ru/TiO_2 prepared by photo-deposition, i.e. Ru/TiO_2-p, exhibits the highest catalytic activity, followed by Ru/TiO_2 prepared by chemical reduction (Ru/TiO_2-c) and then Ru/TiO_2 prepared by wet impregnation (Ru/TiO_2-i) when identical pre-treatment is employed. On the other hand, Ru/TiO_2 pre-treated under H_2–CO atmosphere appears to be more active than that pre-treated under H_2 or CO atmosphere whatever preparation method is employed. Accordingly, Ru/TiO_2-p pre-treated under H_2–CO atmosphere appears to be the most active catalyst for PROX. Typically, CO conversion increased dramatically from 5.4% to 91.4% with increasing reaction temperature from 323 to 333 K, accompanied by the decrease in CO_2 selectivity from 85.1% to 51.2%. The complete removal of CO could be observed at the temperature range of 373–453 K. Although

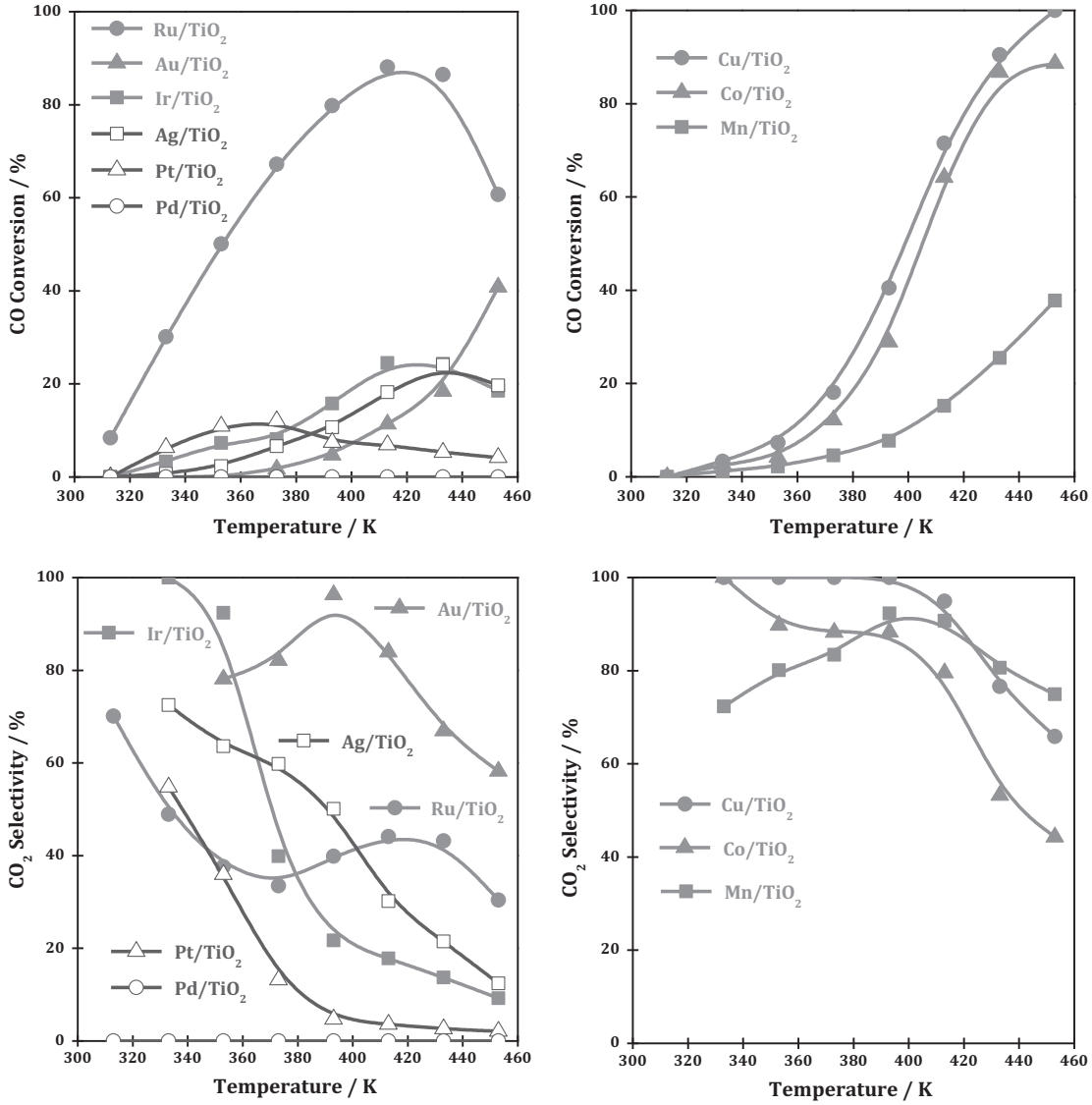

Fig. 1. PROX of CO over TiO_2 supported catalysts prepared by photo-deposition (metal loading: 1% for Ru, Au, Ir, Ag, Pt and Pd; 5% for Cu, Co and Mn). Reaction conditions: 1% CO, 1% O_2, 60% H_2, balanced with He, GHSV = 22,500 h^{-1}.

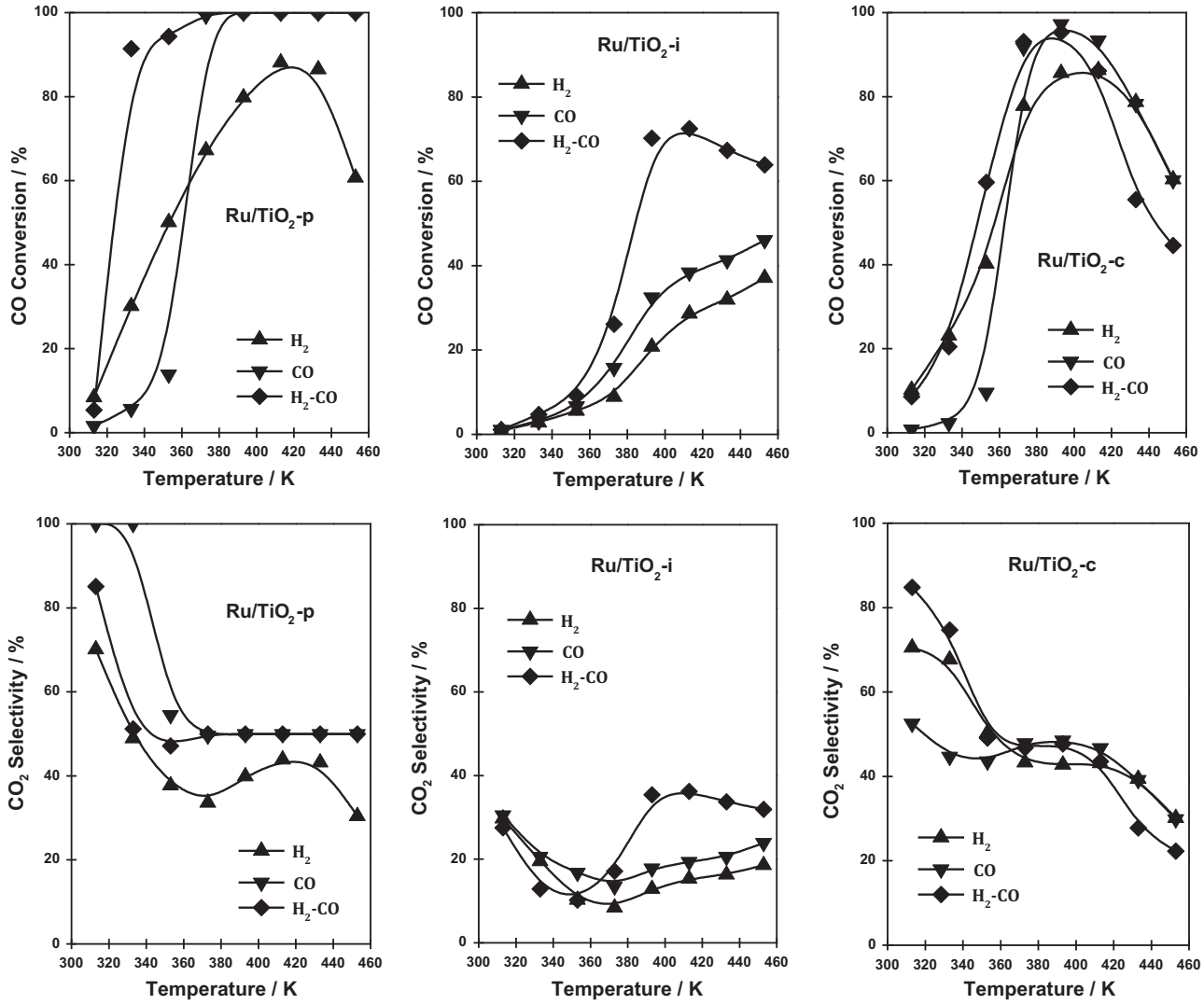

Fig. 2. PROX of CO over Ru/TiO_2: Effects of preparation methods and catalyst pre-treatments. Reaction conditions: 1% CO, 1% O_2, 60% H_2, balanced with He, GHSV = 22,500 h^{-1}.

increasing reaction temperature can greatly enhance the competing oxidation of H_2, the oxidation of CO seems to be selective and CO_2 selectivity of 50% could be obtained at 373–453 K. Based on the catalytic data presented in Fig. 2, Ru/TiO_2-p pre-treated under H_2–CO atmosphere is a very promising PROX catalyst for application in fuel cell since its active temperature window (353–453 K) matches up well with the operation temperature range of fuel cells (353–393 K). Moreover, considering that the chemical composition of catalysts remained unchanged, the different PROX performance of Ru/TiO_2 by different preparation methods and pre-treatment atmospheres should originate from the different existing states and reconstruction of active Ru sites, which will be focused on the following section.

The separate CO oxidation in the absence of H_2 and H_2 oxidation in the absence of CO were examined over Ru/TiO_2-p catalysts, as shown in Fig. 3. As expected, the pre-treatment atmospheres show some impacts on the oxidation of both CO and H_2, due to the construction of Ru sites during treatment (vide infra). For CO oxidation, CO conversion increases with increasing reaction temperature over all Ru/TiO_2-p samples studied and the highest activity is observed for Ru/TiO_2-p pre-treated under H_2 atmosphere, followed by that under H_2–CO and then that under CO. For H_2 oxidation, similar trend could be observed. It appears that pre-treatment under H_2 atmosphere could promote the oxidation of both CO and H_2 to some extent, probably due to the reconstruction of Ru sites induced by H_2. By comparing the CO oxidation over Ru/TiO_2-p in the absence (Fig. 3) and presence of excess H_2 (Fig. 2), we come to the conclusion that the presence of excess H_2 could great promote CO oxidation, which should be associated with the changes in active Ru sites and subsequent reaction mechanism.

The durability of Ru/TiO_2-p catalyst (pre-treated under H_2–CO atmosphere) in PROX is further studied. No changes in both CO conversion and CO_2 selectivity could be observed on Ru/TiO_2-p within 40 h at 373 K, indicating the good stability of catalyst. However in contrast, a slight decrease in both CO conversion (100 to 91.4%) and CO_2 selectivity (50 to 45.7%) did occur in prolonged time-on-stream to 110 h, which should be associated with changes in active Ru sites during reaction (with the presence of both CO and H_2). That is to say, the catalytic deactivation induced by the active sites reconstruction should be considered for Ru and other platinum group metal catalysts in PROX.

3.3. Characterization of Ru/TiO_2 and reconstruction of Ru sites

The surface morphologies of as-prepared Ru/TiO_2-p and samples pre-treated under different reducing atmospheres were

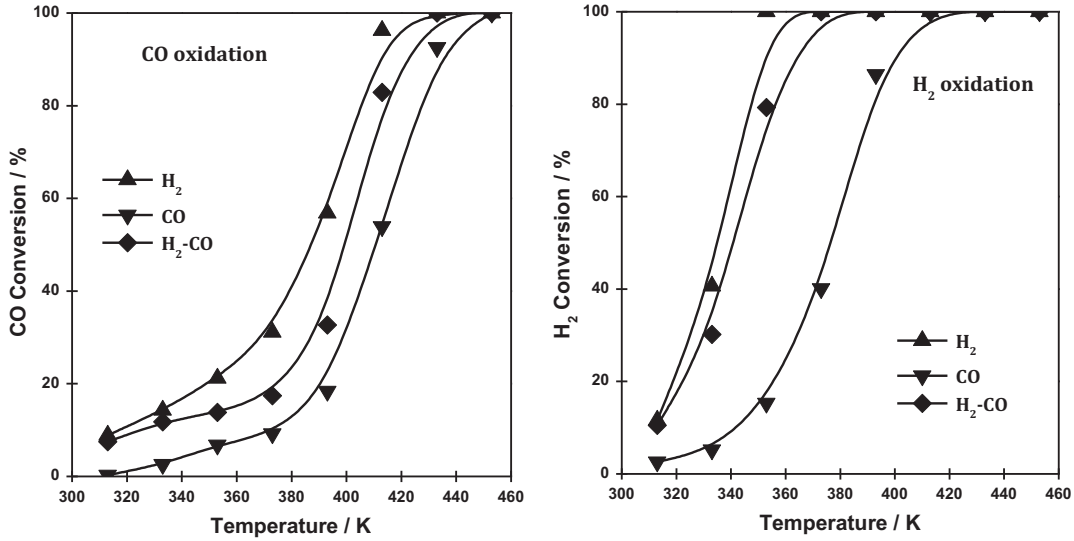

Fig. 3. CO and H_2 oxidation catalyzed by Ru/TiO_2. Reaction conditions: 1% CO or 1% H_2, 1% O_2, balanced with He, GHSV = 22,500 h^{-1}.

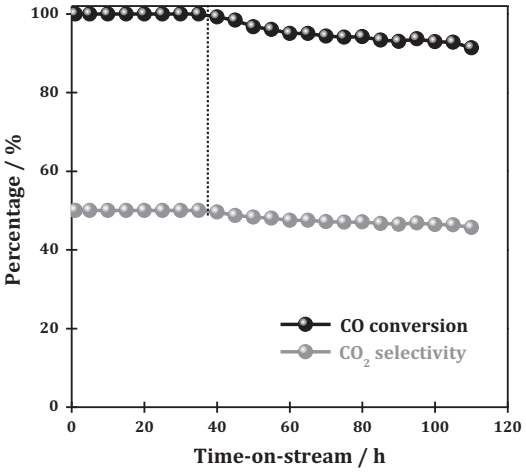

Fig. 4. Time-on-stream behavior of Ru/TiO_2-p in the PROX of CO at 373 K. Reaction conditions: 1% CO, 1% O_2, 60% H_2, balanced with He, GHSV = 22,500 h^{-1}.

investigated and the representative HRTEM images are shown in Fig. 5 (representative images selected from numerous images with statistical validity). For as-prepared Ru/TiO_2-p, no Ru particles could be distinguished in the image although the presence of Ru was confirmed by energy dispersive analysis. This should be due to the high dispersion and probably amorphous structure of Ru species. CO pre-treatment leads to the appearance of spherical nanoparticles with average diameter of ~2 nm, as marked with red circle. H_2 pre-treatment leads to ellipsoidal Ru nanoparticles with fuzzy boundaries and no preferred crystal orientation (average diameter of ~4 nm). Due to the metal-support interaction between Ru and TiO_2, the Ru particles adjacent to TiO_2 spread by covering a layer of support, i.e. TiO_x [25–29]. In great contrast, pre-treatment under H_2–CO produces Ru nanoparticles with clear hexagonal close-packed (HCP) structure (average size of ~3 nm), which is highly active for CO oxidation. It is proposed that the chemisorption of CO occurs on a lattice plane of HCP Ru nanoparticles and the mechanism of CO oxidation with HCP Ru begins with the oxidation of Ru (001) to form a few RuO_2 (110) layers, after which the CO oxidation occurs on RuO_2 (110) [30,31]. Based on the HRTEM observations, it is very clear that different morphologies of Ru nanoparticles could be obtained on TiO_2 support by samples pre-treatment under different reducing atmospheres, which should lead to different metal-support interaction and electron donation between metal and support. A summary of physicochemical prosperities of Ru/TiO_2 catalysts under study is shown in Table 1.

XPS analysis is performed to study the electronic states of Ru/TiO_2-p pre-treated under different reducing atmospheres, and the results are shown in Figs. 6 and 7. In Ti 2p region (Fig. 6), binding energy values at 456.5, 458.5, 461.8 and 464.1 eV could be observed. The binding energy values at 458.5 and 464.1 are attributed to $2p_{3/2}$ and $2p_{1/2}$ of Ti(IV) in TiO_2, respectively, while those at 456.5 and 461.8 eV are attributed to $2p_{3/2}$ and $2p_{1/2}$ of partially reduced Ti species, i.e. Ti(III), in TiO_2, respectively [32,33]. It is obvious that the pre-treatment under reducing atmospheres can result in the reduction of Ti(IV) to Ti(III) to some extent. Since the reduction of TiO_2 support would not occur at such low temperature of 523 K (not shown here), the reduction of Ti(IV) is facilitated by the existence of Ru nanoparticles. In case of Ru/TiO_2 pre-treated under H_2, the H_2 would first reduce Ru surface and then spill over from Ru^0 to adjacent TiO_2 to reduce Ti(IV) to Ti(III) during pre-treatment [27,28]. As a result, a large proportion of Ti(IV) in TiO_2 could be reduced to Ti(III), as proved by XPS results. In contrast, only a very small proportion of Ti(IV) in TiO_2 could be reduced to Ti(III) during pre-treatment under CO, indicating the more difficult reduction of Ti(IV) through CO spillover. It is very interesting to note that in the presence of both H_2 and CO during pre-treatment, a very small proportion of Ti(IV) in TiO_2 could be reduced to Ti(III), similar to that pre-treated under CO alone. It implies that CO would predominantly adsorb on Ru surface and, therefore, hinder the interaction between H_2 and Ru surface and subsequent reduction of adjacent Ti(IV) through spillover.

Fig. 7 shows the Ru 3d XPS of Ru/TiO_2-p catalysts pre-treated under different reducing atmospheres. Due to the interference of the intense binding energy peaks corresponding to C 1s peaks with Ru 3d signals, it is impossible to distinguish the Ru $3d_{3/2}$ binding energy peaks. Fortunately, we can still observe the deconvoluted binging energy values at 279.6, 280.9 and 282.4 eV. The binding energy values at 279.6 and 282.4 eV are attributed to Ru $3d_{5/2}$ of metallic Ru^0 and cationic Ru^{3+}, respectively [34–36]. The binding energy value at 280.9 eV is also due to Ru $3d_{5/2}$ of cationic Ru species, which was proposed to be $Ru^{\delta+}$ species [35]. In a general sense, the reduction of Ru by H_2 or CO should start from the outmost layer to the inner one. That is, metallic Ru clusters should

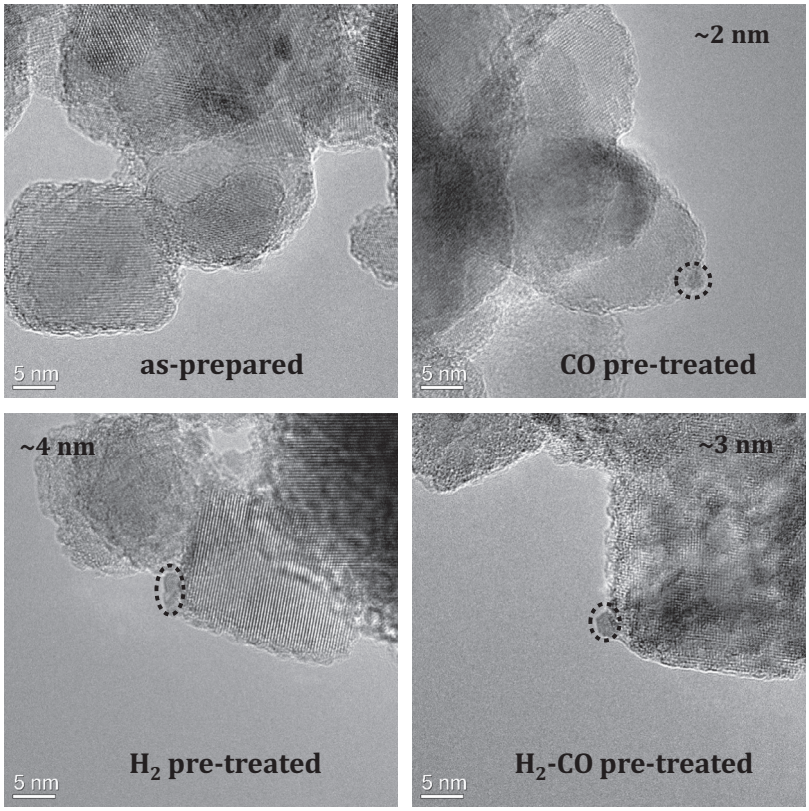

Fig. 5. HRTEM images of as-prepared Ru/TiO_2-p and Ru/TiO_2-p samples pre-treated under different reducing atmospheres. Ru species are marked with circles.

Table 1
Physicochemical prosperities of Ru/TiO_2 catalysts under study.

Catalyst	Pre-treatment atmosphere	Ru loading (%)[a]	Ru dispersion (%)[b]	S_{BET} (m^2/g)[c]	Ru size (nm)[d]
Ru/TiO_2-p	60% H_2	0.93	17.3	44.2	4.1
Ru/TiO_2-p	1% CO	0.96	37.9	47.3	1.9
Ru/TiO_2-p	60% H_2 & 1% CO	0.95	36.2	47.8	3.2
Ru/TiO_2-i	60% H_2	0.91	20.1	46.3	3.5
Ru/TiO_2-i	1% CO	0.93	39.4	47.5	1.6
Ru/TiO_2-i	60% H_2 & 1% CO	0.91	35.2	46.9	3.1
Ru/TiO_2-c	60% H_2	0.94	16.9	42.1	4.2
Ru/TiO_2-c	1% CO	0.96	32.5	44.6	2.8
Ru/TiO_2-c	60% H_2 & 1% CO	0.96	31.7	44.1	3.6

[a] Determined by ICP.
[b] Measured by CO adsorption.
[c] Determined by nitrogen physisorption.
[d] Determined by TEM observations.

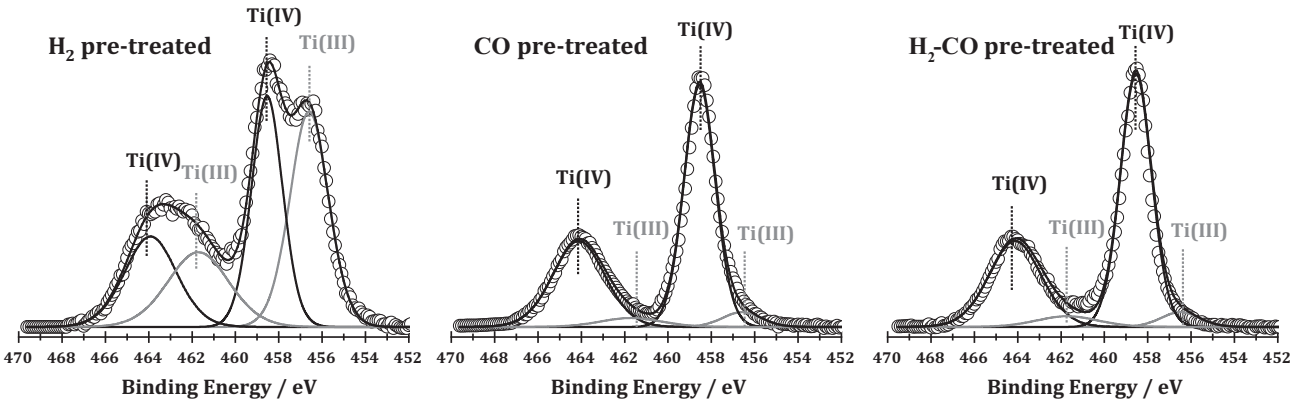

Fig. 6. Ti 2p XPS of Ru/TiO_2-p samples pre-treated under different reducing atmospheres.

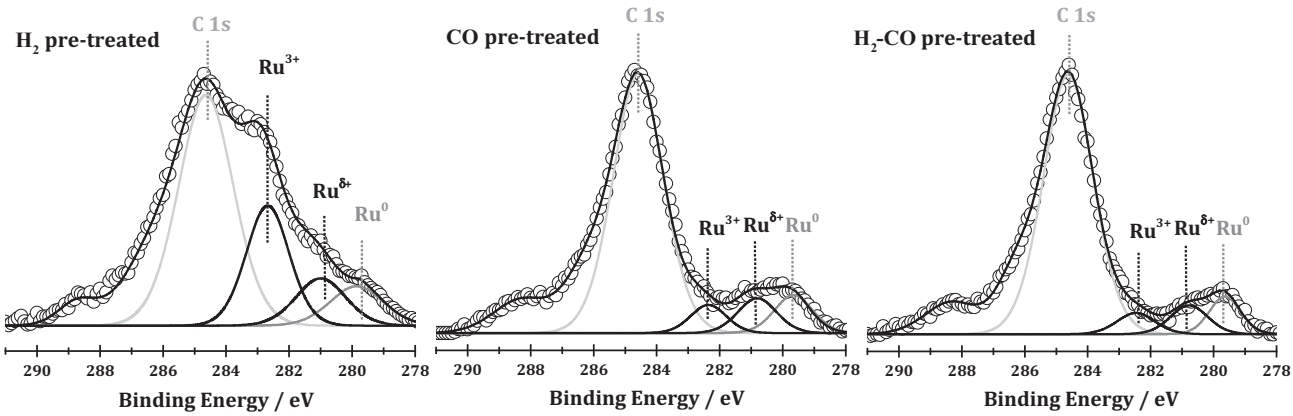

Fig. 7. Ru 3d XPS of Ru/TiO_2-p samples pre-treated under different reducing atmospheres.

be dominant exposed Ru sites, $Ru^{\delta+}$ species locate at the Ru–TiO_2 interface, while cationic Ru^{3+} be buried inside, which is not available during reaction. Based on the XPS results in Fig. 7, distinctly more cationic Ru^{3+} are presented in Ru/TiO_2 pre-treated under H_2 atmosphere, probably due to the so-called strong metal-support interaction formed during pre-treatment [37,38], consistent with TEM observations (Fig. 5). This is further confirmed by the significant lower Ru dispersion in Ru/TiO_2 pre-treated under H_2 (17.3%, Table 1) than that pre-treated under CO (37.9%) or H_2–CO (36.2%).

FTIR spectroscopy with molecular probe is an informative and sensitive technique for the characterization of metal sites. The characteristic of this technique lies in that only exposed sites can be explored, while sites in sub-surface position or buried inside cannot be detected. Thus, it can provide us with necessary information on the available or so-called working sites in catalytic reactions. The FTIR spectra of CO adsorption on Ru/TiO_2-p pre-treated under different reducing atmospheres are shown in Fig. 8. It is seen that IR bands at 2175 and 2115 cm^{-1}, characteristic of CO adsorption on the TiO_2 surface consisting of two types of crystal structures [39], could be observed in all cases and they would not be discussed in this study. For Ru/TiO_2-p pre-treated under CO, CO adsorption at 293 K resulted in the appearance of a very weak IR band at 2060 cm^{-1} and two additional IR bands at 1995 and 1955 cm^{-1} could be observed at higher adsorption temperatures. The bands at 2060 and 1995 cm^{-1} could be attributed to dicarbonyl species adsorbed on reduced Ru crystallites, i.e. $Ru^0(CO)_2$, while the band at 1955 cm^{-1} could be attributed to bridge-bonded carbonyls on reduced Ru crystallites [21,39–41]. With the increase adsorption temperature, the intensities of all the three bands increased gradually, indicating the enhanced adsorption of CO on exposed Ru surfaces. For Ru/TiO_2-p pre-treated under H_2, CO adsorption did not give significant signals corresponding to carbonyls on reduced Ru originally. At higher adsorption temperature of 313–353 K, IR bands at 2060, 2015 and 1995 cm^{-1} could be observed. The IR band at 2015 cm^{-1} is due to linear monocarbonyls on metallic Ru^0 with low nuclearity or surrounded by cationic Ru^{n+} species [40,42]. In another word, these Ru^0 species are rather isolated compared with Ru^0 clusters. Further increase in adsorption temperature (>353 K) resulted in the disappearance of these Ru species and the IR band at 2015 cm^{-1} could not be observed any more. This should be due to the interaction between CO and Ru at high temperatures and subsequent changes in existing states of exposed Ru species. Moreover, the insufficient thermal stability of linear monocarbonyls on metallic Ru^0 should also indicate the high activity of these species. In case of Ru/TiO_2-p pre-treated under H_2–CO, the FTIR spectra of CO adsorption were quite similar with those observed from Ru/TiO_2-p pre-treated under H_2 atmosphere. Based on the FTIR spectra of CO adsorption presented in Fig. 8, we could come to the conclusion that the surface reconstruction of Ru occurred during the catalyst pre-treatments and the surface sites composition depended very much on the pre-treatment atmospheres. According to the kinetic data in Fig. 2, the difference

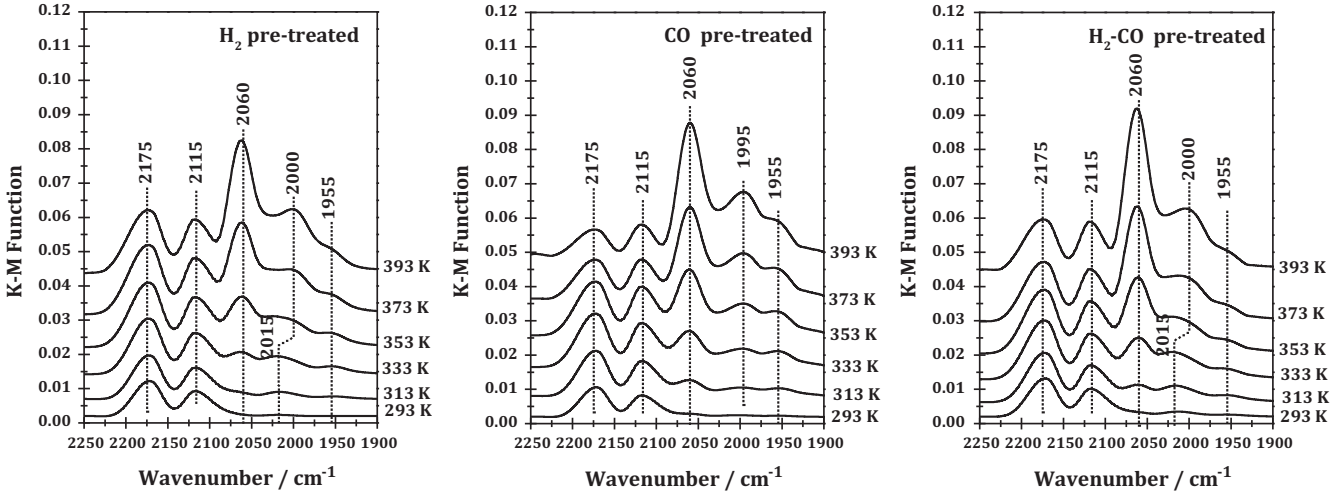

Fig. 8. FTIR spectra of CO adsorption at different temperatures over Ru/TiO_2-p samples pretreated under different reducing atmospheres.

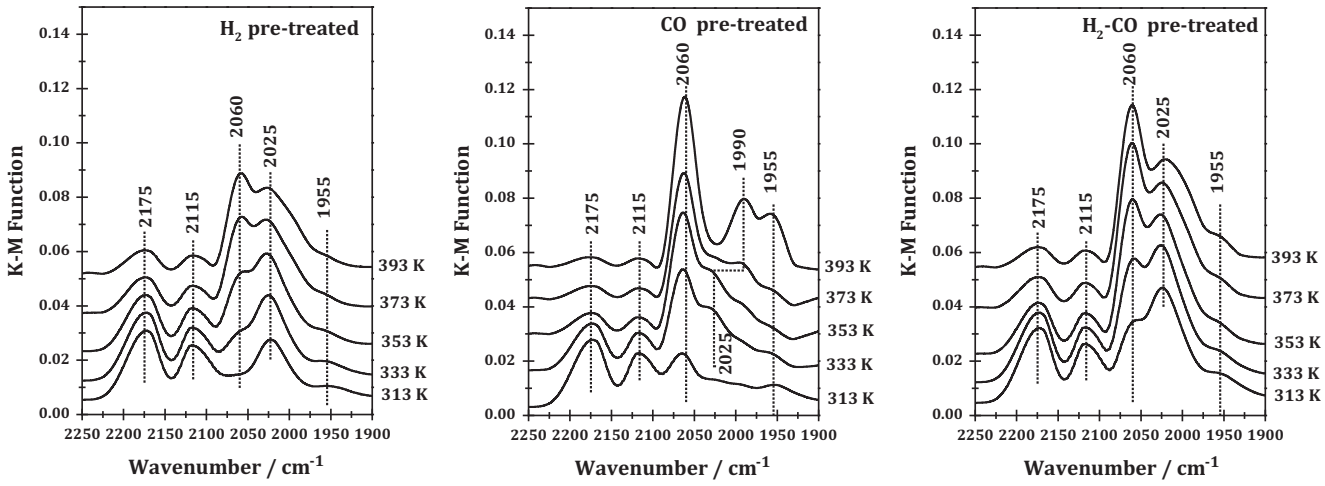

Fig. 9. In site FTIR spectra of PROX over Ru/TiO_2-p samples pretreated under different reducing atmospheres.

in the catalytic activity is quite obvious at low temperature range of 313–353 K over Ru/TiO_2-p pre-treated under different atmospheres. On the other hand, the exposed Ru species probed by FITR spectroscopy of CO adsorption are also quite different in this temperature range. In this context, it is reasonable to propose that isolated Ru^0 species (corresponding to CO adsorption IR band at 2015 cm^{-1}) are associated with the activity difference observed, which will be further explained in the next section.

3.4. Mechanism of PROX catalyzed by Ru/TiO_2

To obtain more information on the reaction process of PROX over Ru/TiO_2, in situ FTIR spectra were recorded and the results are shown in Fig. 9. For Ru/TiO_2-p pre-treated under H_2, linear monocarbonyls on isolated metallic Ru^0 could be observed at 313 K and this band shifted a higher frequency (from 2015 to 2025 cm^{-1}) with the presence of oxygen in the reaction stream. At higher temperatures, dicarbonyl and bridge-bonded carbonyls adsorbed on Ru^0 clusters (IR bands at 2060 and 1955 cm^{-1}, IR bands at 1990 cm^{-1} could not be clearly distinguished due to the overlap with bands at 2025 cm^{-1}) appeared and the intensities corresponding IR bands changed with reaction temperatures. For Ru/TiO_2-p pre-treated under CO, dicarbonyls adsorbed on Ru^0 clusters could be observed at 313 K (IR band at 2060 cm^{-1}) and their concentration (intensity of corresponding IR band) increased with reaction temperature. Weak IR band at 2025 cm^{-1} linear monocarbonyls on metallic Ru^0 appeared at 333 K and it disappeared at 373 K. Meanwhile, a sharp increase in the intensity of IR band at 1955 cm^{-1} corresponding bridge-bonded carbonyls adsorbed on Ru^0 clusters could be observed at 393 K. For Ru/TiO_2-p pre-treated under H_2–CO, linear monocarbonyls on isolated metallic Ru^0 species (IR band at 2025 cm^{-1}), dicarbonyls adsorbed on Ru^0 clusters (IR band at 2060 cm^{-1}) and bridge-bonded carbonyls adsorbed on Ru^0 clusters (IR bands at 1955 cm^{-1}) could be observed at 313 K. With increasing reaction temperature, the concentration of monocarbonyls on isolated metallic Ru^0 decreased while the concentration of dicarbonyls adsorbed on Ru^0 clusters increased instead.

Based on the in situ FTIR spectroscopic results, two types of Ru active sites, i.e. metallic Ru^0 with low nuclearity or surrounded by cationic Ru^{n+} and Ru^0 clusters, and three types of reaction intermediates, i.e. dicarbonyls on Ru^0 clusters, bridge-bonded carbonyls on Ru^0 clusters and monocarbonyls on isolated metallic Ru^0, could be identified. By associating with the spectroscopic observation (Figs. 8 and 9) with kinetic data (Fig. 2), it could be proposed that isolated metallic Ru^0 is the preferred active site for PROX reaction and linear monocarbonyls are more active reaction intermediates. At low reaction temperature range of 333–373 K under kinetic control, Ru/TiO_2-p pre-treated under H_2–CO exhibited higher activity than others with a higher concentration of linear monocarbonyls on isolated metallic Ru^0 (after normalization with IR bands at 2175 and 2115 cm^{-1}).

With Ru/TiO_2-p pre-treated under H_2–CO as a model catalyst, the mechanism of PROX will be further discussed. To derive a reliable mechanism, the following experimental observations should be considered and satisfied: (i) adsorption of CO on Ru sites is always preferred over H_2 (XPS results in Fig. 6); (ii) reconstruction of Ru sites does occur during CO adsorption at 293–393 K (FTIR results in Fig. 8) while no reconstruction could be observed under in situ reaction conditions (FTIR results in Fig. 9); (iii) the presence of H_2 greatly promotes the oxidation of CO (kinetic data in Figs. 2 and 3); (iv) stable CO_2 selectivity of ca. 50% could be observed during PROX reaction at 333–393 K (kinetic data in Fig. 2); (v) no methanation product CH_4 or carbon deposit are formed during reaction; (vi) CO conversion is rather stable at 373 K for within time-on-stream of 40 h and the decrease in CO conversion with prolonged time-on-stream is accompanied by the decrease in CO_2 selectivity (durability data in Fig. 4). According to these important issues, the reaction PROX of CO over isolated metallic Ru^0 is illustrated as follows.

$$Ru + CO \rightarrow Ru - CO; \quad (R1)$$

$$Ru - CO + O_2 \rightarrow CO_2 + Ru - O; \quad (R2)$$

$$Ru - O + H_2 \rightarrow H_2O + Ru. \quad (R3)$$

In the first step, CO adsorb on isolated Ru site to form linear monocarbonyls, which will react with gaseous oxygen to produce CO_2 accompanied by the formation of mono-oxygen covered Ru site (the oxidation of CO promoted by hydroxyl is not discussed in the simplified reaction pathway). The mono-oxygen covered Ru site will then react with gaseous hydrogen and clean Ru site is recovered. In such a way, a complete catalytic cycle is established and CO is oxidized to CO_2 continually. It is clearly seen that equal mole of H_2 and CO is consumed in one catalytic cycle, and, therefore, constant CO_2 selectivity of 50% is observed.

4. Conclusion

A series of TiO_2 supported metal clusters, i.e. Cu, Co, Mn, Pt, Pd, Ir, Ru, Ag and Au, were prepared by photo-deposition and studied

as catalysts in the reaction of CO PROX for fuel cell application. Amongst, Ru/TiO_2 exhibits better catalytic activity in the operation temperature range of fuel cells. Further investigations reveal that the catalyst preparation and pre-treatment show great impacts on the catalytic performance of Ru/TiO_2. Ru/TiO_2 catalyst prepared by photo-deposition and pre-treated under H_2–CO atmosphere is most active in PROX and 100% CO conversion can be obtained at >373 K.

Characterization results from HRTEM, XPS and FTIR spectroscopy of CO adsorption reveal the surface reconstruction during catalyst pre-treatments. Isolated metallic Ru species are identified to be preferred active sites and linear monocarbonyls on isolated metallic Ru species are determined to be key reaction intermediates in PROX. By associating the characterization and catalytic results, the mechanism for PROX is proposed as follows: $Ru + CO \rightarrow Ru - CO$; $Ru - CO + O_2 \rightarrow CO_2 + Ru - O$; $Ru - O + H_2 \rightarrow H_2O + Ru$.

Acknowledgements

This work is financially supported by the Collaborative Innovation Center of Chemical Science and Engineering (Tianjin) and the Ministry of Education of China (IRT-13R30, IRT-13022). The support from 111 Project (B12015) is also acknowledged.

References

[1] Carrette L, Friedrich KA, Stimming U. Fuel cells – fundamentals and applications. Fuel Cells 2001;1:5–39.
[2] Ahmed S, Krumpelt M. Hydrogen from hydrocarbon fuels for fuel cells. Int J Hydrogen Energy 2001;26:291–301.
[3] Song CS. Fuel processing for low-temperature and high-temperature fuel cells challenges, and opportunities for sustainable development in the 21st century. Catal Today 2002;77:17–49.
[4] Dhar HP, Christner LG, Kush AK. Nature of CO adsorption during H_2O oxidation in relation to modeling for CO poisoning of a fuel cell anode. J Electrochem Soc 1987;134(12):3021–6.
[5] Gottesfeld S, Pafford J. A new approach to the problem of carbon monoxide poisoning in fuel cells operating at low temperatures. J Electrochem Soc 1988;135:2651–2.
[6] Springer TE, Rockward T, Zawodzinski TA, Gottesfeld S. Model for polymer electrolyte fuel cell operation on reformate feed effects of CO, H_2 dilution, and high fuel utilization. J Electrochem Soc 2001;148:A11–23.
[7] Trimm DL. Minimisation of carbon monoxide in a hydrogen stream for fuel cell application. Appl Catal A 2005;296:1–11.
[8] Korotkikh O, Farrauto R. Selective catalytic oxidation of CO in H_2: fuel cell applications. Catal Today 2000;62:249–54.
[9] Park ED, Lee D, Lee HC. Recent progress in selective CO removal in a H_2-rich stream. Catal Today 2009;139:280–90.
[10] Oh SH, Sinkevitch RM. Carbon monoxide removal from hydrogen-rich fuel cell feed streams by selective catalytic oxidation. J Catal 1993;142:254–62.
[11] Kahlich MJ, Gasteiger HA, Behm RJ. Kinetics of the selective CO oxidation in H_2-rich gas on Pt/Al_2O_3. J Catal 1997;171:93–105.
[12] Son IH, Shamsuzzoha M, Lane AM. Promotion of Pt/γ-Al_2O_3 by new pretreatment for low-temperature preferential oxidation of CO in H_2 for PEM fuel cells. J Catal 2002;210:460–5.
[13] Huang Y, Wang A, Wang X, Zhang T. Preferential oxidation of CO under excess H_2 conditions over iridium catalysts. Int J Hydrogen Energy 2007;32:3880–5.
[14] Liu K, Wang AQ, Zhang T. Recent advances in preferential oxidation of CO reaction over platinum group metal catalysts. ACS Catal 2012;2:1165–78.
[15] Kahlich MJ, Gasteiger HA, Behm RJ. Kinetics of the selective low-temperature oxidation of CO in H_2-rich gas over Au/α-Fe_2O_3. J Catal 1999;182:430–40.
[16] Bethke GK, Kung HH. Selective CO oxidation in a hydrogen-rich stream over Au/γ-Al_2O_3 catalysts. Appl Catal A 2000;194:43–5.
[17] Wang JB, Lin SC, Huang TJ. Selective CO oxidation in rich hydrogen over CuO/samaria-doped ceria. Appl Catal A 2002;232:107–20.
[18] Teng Y, Sakurai H, Ueda A, Kobayashi T. Oxidative removal of CO contained in hydrogen by using metal oxide catalysts. Int J Hydrogen Energy 1999;24:355–8.
[19] Yen H, Seo Y, Kaliaguine S, Kleitz F. Tailored mesostructured copper/ceria catalysts with enhanced performance for preferential oxidation of CO at low temperature. Angew Chem Int Ed 2012;124:12198–201.
[20] Echigo M, Tabata T. A study of CO removal on an activated Ru catalyst for polymer electrolyte fuel cell applications. Appl Catal A 2003;251:157–66.
[21] Chin SY, Alexeev OS, Amiridis MD. Preferential oxidation of CO under excess H_2 conditions over Ru catalysts. Appl Catal A 2005;286:157–66.
[22] Kim YH, Park ED, Lee HC, Lee D. Selective CO removal in a H_2-rich stream over supported Ru catalysts for the polymer electrolyte membrane fuel cell (PEMFC). Appl Catal A 2009;366:363–9.
[23] Wu G, Guan N, Li L. Low temperature CO oxidation on $Cu–Cu_2O/TiO_2$ catalyst prepared by photo-deposition. Catal Sci Technol 2011;1:601–8.
[24] Li L, Qu L, Cheng J, Li J, Hao Z. Oxidation of nitric oxide to nitrogen dioxide over Ru catalysts. Appl Catal B 2009;88:224–31.
[25] Komaya T, Bell AT, WengSieh Z, Gronsky R, Engelke F, King TS, et al. The influence of metal-support interactions on the accurate determination of Ru dispersion for Ru/TiO_2. J Catal 1994;149:142–8.
[26] Shen XF, Garces LJ, Ding YS. Behavior of H_2 chemisorption on Ru/TiO_2 surface and its application in evaluation of Ru particle sizes compared with TEM and XRD analyses. Appl Catal A 2008;335:187–95.
[27] Pham TN, Shi D, Sooknoi T, Resasco DE. Aqueous-phase ketonization of acetic acid over Ru/TiO_2/carbon catalysts. J Catal 2012;295:169–78.
[28] McQuire MW, Rochester CH. FTIR study of CO/H_2 reactions over Ru/TiO_2 and $Ru–Rh/TiO_2$ catalysts at high temperature and pressure. J Catal 1995;157:396–402.
[29] Panagiotopoulou P, Kondarides DI, Verykios XE. Mechanistic study of the selective methanation of CO over Ru/TiO_2 catalyst: identification of active surface species and reaction pathways. J Phys Chem C 2011;115:1220–30.
[30] Kusada K, Kobayashi H, Yamamoto T, Matsumura S, Sumi N, Sato K, et al. Discovery of face-centered-cubic ruthenium nanoparticles: facile size-controlled synthesis using the chemical reduction method. J Am Chem Soc 2013;135:5493–6.
[31] Reuter K, Scheffler M. Composition and structure of the $RuO_2(1\,1\,0)$ surface in an O_2 and CO environment: implications for the catalytic formation of CO_2. Phys Rev B 2003;68:045407.
[32] Wagner CD, Riggs WM, Davis LE, Moulder JF, Muilenberg GE. Handbook of X-ray photoelectron spectroscopy: a reference book of standard data for use in X-ray photoelectron spectroscopy. Eden-Prairie, MN: Perkin–Elmer; 1979.
[33] Feng W, Wu G, Li L, Guan N. Solvent-free selective photocatalytic oxidation of benzyl alcohol over modified TiO_2. Green Chem 2011;13:3265–72.
[34] Elmasides C, Kondarides DI, Neophytides SG, Verykios XE. Partial oxidation of methane to synthesis gas over Ru/TiO_2 catalysts: effects of modification of the support on oxidation state and catalytic performance. J Catal 2001;198:195–207.
[35] Nozawa T, Mizukoshi Y, Yoshida A, Naito S. Aqueous phase reforming of ethanol and acetic acid over TiO_2 supported Ru catalysts. Appl Phys B 2014;146:221–6.
[36] Sayan S, Süzer S, Uner DO. XPS and in-situ IR investigation of $Ru/Si0_2$ catalyst. J Mol Struct 1997;410–411:111–4.
[37] Tauster SJ, Fung SC, Garten RL. Strong metal-support interactions group 8 noble metals supported on TiO_2. J Am Chem Soc 1978;100:170–5.
[38] Tauster SJ, Fung SC, Baker RTK, Horsley JA. Strong interactions in supported-metal catalysts. Science 1981;211:1121–5.
[39] Hadjiivanov K, Lavalley JC, Lamotte J, Maugé F, Saint-Just J, Che M. FTIR study of CO interaction with Ru/TiO_2 catalysts. J Catal 1998;176:415–25.
[40] Chin SY, Williams CT, Amiridis MD. FTIR studies of CO adsorption on Al_2O_3 and SiO_2 supported Ru catalysts. J Phys Chem B 2006;110:871–82.
[41] Mizushima T, Tohji K, Udagawa Y, Ueno A. EXAFS and IR study of the CO-adsorption induced morphology change in Ru catalysts. J Am Chem Soc 1990;112:7887–93.
[42] Elmasides C, Kondarides DI, Grünert W, Verykios XE. XPS and FTIR study of Ru/Al_2O_3 and Ru/TiO_2 catalysts: reduction characteristics and interaction with a methane oxygen mixture. J Phys Chem B 1999;103:5227–39.